Research Square

Preprints are preliminary reports that have not undergone peer review.
They should not be considered conclusive, used to inform clinical practice,
or referenced by the media as validated information.

A Cyber-Physical Readiness Framework for Robot-Assisted Surgery: Scenario-Based Assessment of XR and Teleoperation

Unais Ali

unais@umich.edu

Eastern Michigan University

Muhammad Ahmed

Eastern Michigan University

Syeda Kashaf Kulsoom

UTech Digital Education

Research Article

Keywords: robot-assisted surgery, cyber-physical systems, extended reality, teleoperation, readiness framework, multi-criteria analysis

Posted Date: November 3rd, 2026

DOI: https://doi.org/10.21203/rs.3.rs-11531265/v1

License: This work is licensed under a Creative Commons Attribution 4.0 International License.
Read Full License

Additional Declarations: No competing interests reported.

A Cyber-Physical Readiness Framework for Robot-Assisted Surgery: Scenario-Based Assessment of XR and Teleoperation

Unais Ali[1*], Muhammad Ahmed[1] and Syeda Kashaf Kulsoom[2]

[1*]College of Technology, Eastern Michigan University, Ypsilanti, 48197, MI, United States.

[2]UTech Digital Education, Karachi, Pakistan.

*Corresponding author(s). E-mail(s): uali@emich.edu;
Contributing authors: mahmed6@emich.edu; kashaf@utech-edu.com;

Abstract

Robot-assisted surgery requires more than an operative console: clinical deployment depends on instruments, visualization and extended reality (XR), network reliability, team training, credentialing, and governance. This study develops a five-layer cyber-physical readiness framework for comparing elective robot-assisted surgery, XR-focused robotic training, and networked teleoperation. A weighted multi-criteria index combines literature-informed layer scores for console control, instruments, vision/XR, network capability, and governance. The model includes scenario-dependent weights, an illustrative model threshold, and a teleoperation safety gate requiring acceptable latency, authentication, fail-safe stopping, local recovery capability, and clear credentialing and liability arrangements. Under the coded illustrative inputs, elective robot-assisted surgery meets the model threshold ($\boldsymbol{R = 0.736}$), XR-focused training lies near it ($\boldsymbol{R = 0.674}$), and remote teleoperation remains below it ($\boldsymbol{R = 0.619}$) and fails the safety gate. Sensitivity and uncertainty analyses identify network assurance, fail-safe coverage, console performance, and governance as high-leverage factors. The framework is a transparent program-level decision aid; it is not a validated clinical prediction model, regulatory score, or substitute for procedure- and site-specific safety assessment.

Keywords: robot-assisted surgery, cyber-physical systems, extended reality, teleoperation, readiness framework, multi-criteria analysis

1 Introduction and Contributions

Robot-assisted surgery (RAS) is no longer a niche demonstration technology. Over three decades it has moved from early master-slave concepts and market-driven acquisition debates [3, 13] to multi-specialty clinical platforms with three-dimensional vision, wristed instruments, and expanding hospital footprints [20, 29]. Program leaders nevertheless still lack a compact quantitative answer to a practical question: for *this* scenario: elective console surgery, extended reality (XR)-supported robotic training, or networked teleoperation, are console control, instruments, vision/XR, network integrity, and credentialing jointly adequate? Platform reviews, soft-robot surveys, XR education syntheses, and clinical trials each illuminate one facet [12, 17, 20, 26], but they rarely produce a computable readiness index with transparent weights, sensitivity, and hard failure gates. This paper closes that gap with an operating room (OR)-native multi-criteria cyber-physical system (CPS) readiness model for *Journal of Robotic Surgery*.

The remainder of the paper is linked as follows. Section 1 reviews the evidence corpus that motivates five OR layers. Section 2 answers research question 1 (RQ1) by defining the readiness index $R^{(c)}$, threshold, and teleoperation gate. Section 3 answers research question 2 (RQ2) by computing scenario scores, threshold sensitivity, and local/Dirichlet weight sensitivity. Section 4 deepens RQ2 with uncertainty, upgrade prioritization, and illustrative feature ranking. Section 5 interprets the answers for clinical programs, and Section 6 restates the RQ answers and limitations.

1.1 Literature review: platforms, outcomes, soft systems, XR, and teleoperation

Platform evolution and adoption.

Early reviews framed robotic surgery as technologically promising yet clinically immature, with limited comparative cost–benefit data relative to conventional techniques [3]. Subsequent historical surveys traced telepresence concepts through commercial multiport systems and highlighted curriculum, haptics, and cost as persistent readiness bottlenecks [13]. Contemporary technology reviews catalogue U.S. Food and Drug Administration (FDA)–cleared and emerging platforms, emphasizing that competitive console and instrument ecosystems must be scored as systems, not as single devices [20]. Population data confirm rapid diffusion once hospitals purchase robots: robotic shares of common procedures rose sharply over a few years, even when evidence for superiority remained procedure-dependent [29]. Anatomic technique innovations such as completely intrafascial approaches further show that platform capability and surgical workflow co-evolve [9]. Flexible and continuum architectures extend this trajectory toward single-port and confined-space access [30, 40].

Randomized and synthesized clinical evidence.

High-level evidence now clarifies where RAS changes perioperative risk and where it does not. In rectal cancer, the Robotic versus Laparoscopic Resection for Rectal Cancer (ROLARR) trial found robotic assistance non-inferior to laparoscopy on conversion risk in a multicenter randomized controlled trial (RCT) design [17]. In prostatectomy,

early and 24-month randomized comparisons versus open surgery report similar functional recovery patterns while refining oncologic interpretation [11, 21]; continence meta-analyses further quantify functional recovery ranges after robot-assisted radical prostatectomy [10]. For bladder cancer, the iROC RCT showed more days alive and out of hospital after robot-assisted cystectomy with intracorporeal diversion versus open surgery, alongside fewer selected wound and thromboembolic events [42]. Esophagectomy and oropharyngeal trials similarly position RAS within specialty-specific morbidity and quality-of-life (QOL) trade-offs [24, 28]. Overview-of-reviews work cautions that broad claims of universal clinical superiority are not supported: benefits are procedure-specific and often modest relative to adoption intensity [32]. These findings motivate readiness scoring that separates *technical platform maturity* from *outcome-justified deployment*.

Soft, continuum, and intelligent effectors.

Beyond rigid wristed tools, soft and continuum robots promise safer interaction with deformable anatomy. Biomedical soft-robotics reviews map materials, actuation, and clinical use-cases spanning surgery and assistance [22]. Minimally invasive surgery (MIS)-focused surveys compare design families and argue for structured evaluation of sterilization, sensing, and control before routine OR use [26]. Actuator and manipulator surveys detail inflatable elastic actuators, stiffness tuning, and sensing needed for compliant manipulation [18, 35], while intelligent soft surgical robot roadmaps emphasize autonomy-aware control and next-generation MIS platforms [36]. Continuum manipulation surveys and miniature soft locomotion reviews expand the design space for navigation in constrained cavities [30, 31]; origami soft crawlers illustrate magnetically actuated confined-space mobility [43]. Flexible robotic MIS reviews synthesize kinematics, constraint control, and clinical status for single-port pathways relevant to Layer 2 scoring [40].

Surgical education, XR, and skill transfer.

Skills laboratories and simulation are now recognized as infrastructure, not optional add-ons: motor learning theory and duty-hour pressures pushed basic skills out of the live OR [4]. Classic randomized evidence showed that virtual reality (VR) training to expert criteria reduces operative errors and improves dissection efficiency [2]. Systematic reviews of augmented reality (AR) medical training and meta-analyses of VR for health-professions education report knowledge and skill gains but uneven methodological quality and transfer validation [12, 25]. Head-mounted XR reviews and broader clinical VR surveys similarly stress application-specific fidelity requirements for surgical rehearsal versus general education [14, 37]. Metaverse-oriented educational analyses extend this discussion to persistent multi-user virtual learning environments and their limits [38]. Teaching-by-demonstration methods for robot-assisted MIS further link recorded human demonstrations to robot skill models under remote center of motion (RCM) constraints [33], while deep imitation learning from consumer VR teleoperation shows how XR interfaces can generate training data for complex manipulation policies [19].

Teleoperation theory, haptics, human factors, and autonomy.

Force-reflecting teleoperation under delay has a rigorous control heritage: passivity and wave-variable formulations stabilize delayed bilateral loops [1]. In clinical robot-assisted minimally invasive surgery (RMIS), lack of high-fidelity haptic feedback remains a central human–machine limitation [7]. Human-performance reviews for teleoperated robots document situation awareness loss, video bandwidth limits, lag, and frame-of-reference switching, and recommend multimodal and predictive interfaces [5]. Learning-based force-sensorless admittance teleoperation offers compliant interaction without dedicated force/torque sensing [34]. Autonomy taxonomies and standards discussions argue that surgical robots must progress through supervised levels with transparent benchmarks rather than leaping to unsupervised clinical control [23]; in vivo autonomous laparoscopic anastomosis demonstrates frontier capability while underscoring governance needs [41]. Networked OR pathways also sit within the broader Internet of Things (IoT) and Industry 4.0 convergence of connected devices, market adoption pressure, and cyber-physical risk management documented across two decades of IoT research [44].

Adjacent cyber-physical training evidence.

Outside the OR, robot-assisted rehabilitation RCTs and reviews show that intensive human–robot training loops can be protocolized and scored against motor endpoints [6, 8, 15, 16, 27, 39]. We cite this only as adjacent evidence that structured robotic curricula can be measured; these sources are not surgical outcome substitutes and do not enter patient-level claims in this framework.

Synthesis and gap.

Across this corpus, five themes recur: (i) console and instrument platforms are comparatively mature for elective RAS [13, 20]; (ii) clinical benefit is procedure-specific and must not be inferred from adoption alone [17, 29, 32, 42]; (iii) soft/flexible effectors remain translationally incomplete relative to rigid tools [26, 36, 40]; (iv) XR can transfer skill when curricula are criterion-based, yet routine AR registration and broad educational validation remain uneven [2, 12, 25, 37]; and (v) remote teleoperation and autonomy are limited by delay, haptics, human factors, fail-safes, and standards [1, 5, 7, 23, 41]. What is missing is a single transparent index that combines these layers for scenario comparison. That is the modeling target of this paper.

1.2 Research questions and contributions

This paper addresses exactly two research questions (RQs):

- **RQ1:** How can robotic OR capability be formalized as a multi-layer readiness score $R^{(c)}$ with scenario-dependent weights and measurable layer scores?
- **RQ2:** Under literature-coded inputs drawn from the curated RAS/XR/soft-robotics/teleoperation corpus used here, how do elective RAS, XR robotic training, and remote teleoperation compare on $R^{(c)}$, and which layers and engineering features most affect the score?

Contributions.

(1) We define a five-layer cyber-physical readiness framework for RAS with explicit equations, an illustrative model threshold, a numeric teleoperation latency parameter, and a binary safety product G. (2) We publish literature-informed indicator coding anchored to the curated corpus, compute scenario readiness with worked arithmetic, run threshold/weight/noise sensitivity, and report adoption-growth statistics from published registry endpoints [29]. (3) We report an illustrative feature-ranking visualization and interpret results for robotic program planning: under the coded inputs, elective RAS meets the illustrative model threshold, whereas remote teleoperation remains below it and is constrained by network and fail-safe layers. Autonomy enters as a governance and safety consideration, not as an unsupervised clinical controller [23, 41].

Evidence corpus.

All bibliographic entries are taken from the authors' curated PDF set (local project folder `new papers`) spanning RAS platforms, clinical RCTs and syntheses, soft/flexible robotics, XR education, teleoperation/autonomy, and IoT/Industry 4.0 networked-systems context [44]; duplicate PDF copies of the same article are cited once.

The literature themes above map directly onto the five layers formalized next: console and instruments (platform maturity), vision/XR (training and guidance), network (teleoperation), and governance (credentialing, standards, and cybersecurity).

2 Model Formulation

This section answers RQ1: we formalize robotic OR capability as a weighted readiness score with an illustrative model threshold and a teleoperation safety gate.

2.1 Layered robotic OR representation

Definition 1 (Robotic OR layers) Let the robotic OR be described by five layers L_i, $i = 1, \ldots, 5$:

1. L_1: console and human control (ergonomics, tremor filtering, control fidelity);
2. L_2: instruments and soft effectors (articulation, compliance, port access);
3. L_3: vision and XR guidance (stereo endoscopy, AR registration, VR training fidelity);
4. L_4: network and teleoperation link (latency, authentication, redundancy);
5. L_5: team, credentialing, and governance (training, liability, cybersecurity process).

Figure 1 summarizes the stack. Soft, continuum, and flexible effectors enter primarily through L_2 [18, 22, 26, 30, 31, 35, 36, 40, 43]; XR training, AR guidance, and demonstration-based skill transfer enter through L_3 [2, 4, 12, 14, 19, 25, 33, 37, 38]; networked remote control, haptics, human factors, and autonomy constraints enter through L_1, L_4, and L_5 [1, 5, 7, 20, 23, 34, 41, 44].

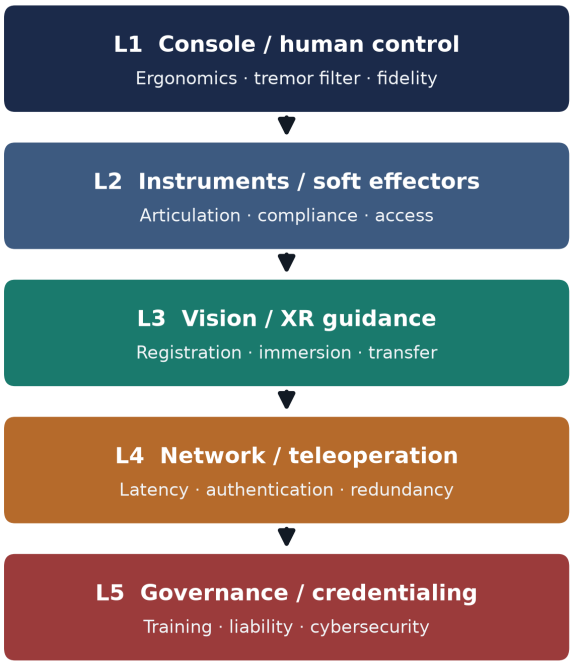


Fig. 1 Five-layer cyber-physical readiness model for the robotic OR (console, instruments, vision/XR, network, governance).

2.2 Readiness index

Definition 2 (Scenario readiness) For clinical scenario $c \in \mathcal{C} = \{\text{elective RAS, XR training, teleoperation}\}$, let $w^{(c)} \in \mathbb{R}^5_{\geq 0}$ be weights and $s^{(c)} \in [0,1]^5$ be layer scores. The readiness index is

$$R^{(c)} = \sum_{i=1}^{5} w_i^{(c)} s_i^{(c)}, \qquad \sum_{i=1}^{5} w_i^{(c)} = 1. \tag{1}$$

Definition 3 (Illustrative model threshold) A scenario is said to *meet the illustrative model threshold* under this model if

$$R^{(c)} \geq \tau, \qquad \tau = 0.70. \tag{2}$$

The threshold $\tau = 0.70$ is an author-chosen illustrative cutoff for comparative analysis, not a validated clinical, regulatory, or patient-level readiness standard. Classifications relative to τ are therefore scenario-model outputs only.

Layer scores $s_i^{(c)}$ are obtained by averaging K_i binary or scaled indicators $x_{ik} \in [0,1]$ coded from published technical and clinical descriptions:

$$s_i^{(c)} = \frac{1}{K_i} \sum_{k=1}^{K_i} x_{ik}^{(c)}. \tag{3}$$

Table 1 lists the indicators and elective-RAS codes used in this study; XR-training and teleoperation scores follow the same template with scenario-adjusted values (Fig. 2). Codes are single-rater author judgments anchored to the cited literature (preliminary proof-of-concept), not multi-rater Delphi estimates or hospital telemetry; no inter-rater agreement statistics are reported.

Table 1 Indicator coding for elective RAS layer scores s_i (each $x_{ik} \in [0,1]$; $s_i = \text{mean}_k x_{ik}$). Anchors are papers in the curated corpus.

Layer	Indicator x_{ik}	Code	Anchor
L_1	Tremor filtering / stability	0.90	[3, 20]
L_1	Console ergonomics / control fidelity	0.85	[7, 13, 20]
L_1	Stereoscopic visualization at console	0.83	[13, 20]
L_2	Articulated wristed instruments	0.95	[9, 13, 20]
L_2	Multi-port / single-port / flexible access options	0.90	[20, 30, 40]
L_2	Soft-compliance maturity for routine use	0.61	[22, 26, 35, 36]
L_3	Endoscopic vision adequacy (non-XR)	0.85	[20]
L_3	AR registration readiness for routine OR	0.45	[12, 14]
L_3	VR curriculum transfer evidence	0.35	[2, 4, 25, 37]
L_4	On-premises wired reliability (elective)	0.70	[1, 20]
L_4	Authenticated / supervised remote session controls	0.35	[5, 23, 44]
L_4	Redundant fail-over / safe autonomy stop	0.15	[23, 41]
L_5	Formal credentialing pathway	0.80	[4, 13, 29]
L_5	Team training / simulation access	0.75	[2, 27, 37]
L_5	Standards-aware safety / autonomy governance	0.60	[23, 32, 41]

Layer means for elective RAS are therefore $s = (0.86, 0.82, 0.55, 0.40, 0.72)$, matching Fig. 2. Weights $w^{(c)}$ encode relative clinical priority (Table 2).

Table 2 Scenario weights $w^{(c)}$ (rows sum to 1)

Scenario	w_1	w_2	w_3	w_4	w_5
Elective RAS	0.28	0.26	0.14	0.08	0.24
XR training	0.12	0.10	0.38	0.08	0.32
Teleoperation	0.22	0.18	0.16	0.24	0.20

Figure 2 plots the same weights beside the scenario layer scores used in all readiness calculations.

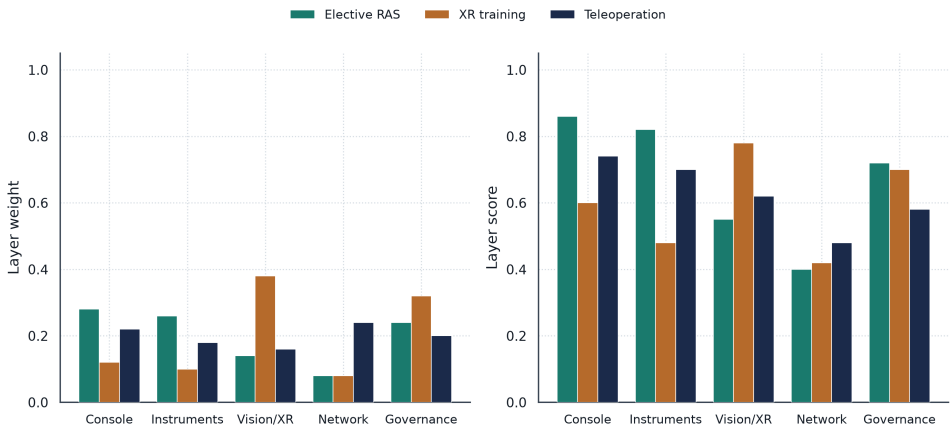


Fig. 2 Scenario weights (left) and literature-coded layer scores (right) used in Eq. (1).

2.3 Teleoperation safety gate

Weighted averaging alone can hide a single catastrophic failure mode. For remote teleoperation we therefore impose both a latency inequality and a binary product gate. Let ℓ denote one-way control/feedback latency. We use a scenario-model latency parameter

$$\ell \le \ell_{\max}, \qquad \ell_{\max} = 150 \text{ ms}, \tag{4}$$

informed by delayed teleoperation stability theory [1], human-performance limits under lag and bandwidth constraints [5], and autonomy/teleoperation safety discussions [23, 41]. It is *not* asserted as a universal validated remote-surgery clinical standard; sites may tighten or relax $\ell_{\max}$ for anatomy, procedure, and network design. Five binary constraints $c_j \in \{\text{pass}, \text{fail}\}$ are then required:

$$G = \prod_{j=1}^{5} \mathbf{1}[c_j = \text{pass}], \qquad \text{remote RAS allowed in the model only if } G = 1 \text{ and (4) holds.} \tag{5}$$

The five constraints are: latency limit (4), authentication integrity, fail-safe stop, local recovery capability, and credentialing/liability clarity (Fig. 3; Table 3). Authentication integrity is interpreted in the IoT/Industry 4.0 sense of trustworthy connectivity, identity, and cyber-physical assurance for networked clinical systems [44]. Under the coded teleoperation inputs we set $c = (\text{fail}, \text{fail}, \text{fail}, \text{fail}, \text{pass})$ for a typical non-dedicated wide-area link lacking proven fail-safe and recovery drills, hence $G = 0$ even before comparing $R^{(c)}$ with τ. Even if $R^{(c)}$ were near τ, $G = 0$ vetoes routine remote operation in this framework [7, 23, 34, 41].

Table 3 Operational definitions for teleoperation gate conditions (pass requires documented evidence)

Gate condition	Pass evidence (examples)	Fail evidence (examples)
Latency $\ell \leq \ell_{\max}$	Measured one-way control/feedback latency within the site-chosen $\ell_{\max}$ on the intended path	Unmeasured latency, or measured $\ell > \ell_{\max}$ on production path
Authentication integrity	Mutual authentication, session integrity checks, and logged identity for console and bedside nodes [44]	Open/shared credentials, unsigned sessions, or no audit trail
Fail-safe stop	Tested emergency stop that leaves instruments in a safe state under link loss [23, 41]	No tested stop, or stop leaves uncontrolled motion risk
Local recovery	On-site surgeon/team can convert or complete care without the remote link [7, 34]	No local recovery plan, staffing, or equipment
Credentialing/liability	Written privileges, cross-site credentialing, and liability/coverage agreements	Informal remote assistance without privileges or liability clarity

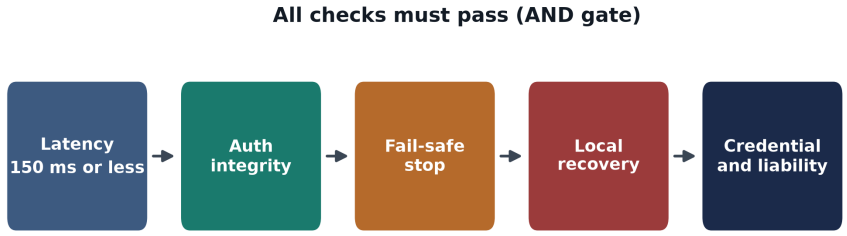


Fig. 3 Teleoperation safety gate: illustrative latency parameter (150 ms or less in this scenario model), authentication, fail-safe stop, local recovery, and credentialing/liability must all pass ($G = 1$ in Eq. (5)).

2.4 Adoption growth statistic

Let p_{t_0} and p_{t_1} be robotic approach shares at years t_0 and t_1. An implied continuous growth rate is

$$\hat{g} = \frac{1}{t_1 - t_0} \ln \frac{p_{t_1}}{p_{t_0}}. \tag{6}$$

Using Sheetz *et al.* endpoints $p_{2012} = 0.018$ and $p_{2018} = 0.151$,

$$\hat{g} = \frac{1}{2018 - 2012} \ln \frac{0.151}{0.018} = \frac{1}{6} \ln(8.3889) \approx 0.354 \text{ yr}^{-1} \tag{7}$$

(Fig. 4). Rapid diffusion motivates readiness scoring: volume growth does not imply layer balance [29].

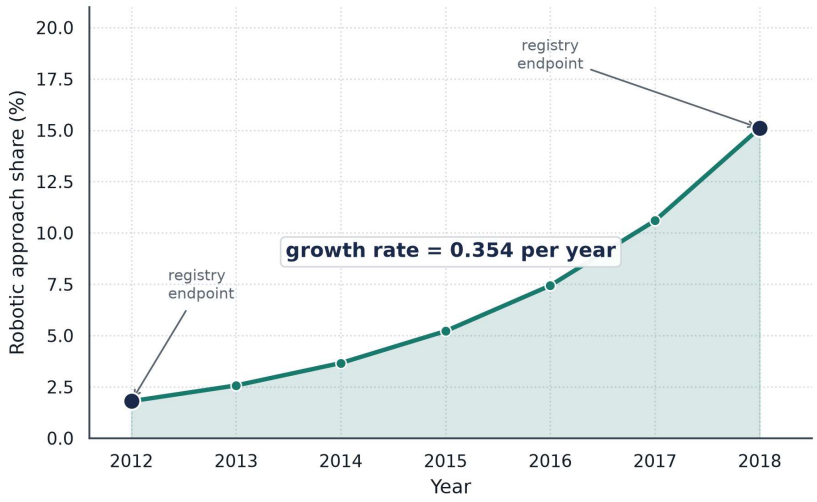


Fig. 4 Robotic approach share for common procedures in a Michigan registry cohort, 2012 (1.8%) and 2018 (15.1%), redrawn from Sheetz *et al.* [29]; implied growth rate from Eq. (6).

3 Correctness Properties and Numerical Analysis

Having defined the index in Section 2 (RQ1), this section answers RQ2 for the three coded scenarios: compute $R^{(c)}$, compare each value with τ, and probe teleoperation weight sensitivity.

3.1 Basic correctness properties

Proposition 1 (Boundedness) *If* $w_i^{(c)} \geq 0$, $\sum_i w_i^{(c)} = 1$, *and* $s_i^{(c)} \in [0,1]$, *then* $R^{(c)} \in [0,1]$.

Proof $R^{(c)}$ is a convex combination of values in $[0,1]$, hence lies in $[0,1]$. □

Proposition 2 (Monotonicity) *Fix* $w^{(c)}$. *If* $s^{(c)} \leq \tilde{s}^{(c)}$ *componentwise, then* $R^{(c)} \leq \tilde{R}^{(c)}$.

Proof Immediate from non-negative weights in Eq. (1). □

These properties ensure that improving any layer never decreases readiness and that scores remain interpretable on a unit interval.

3.2 Computed readiness (RQ1–RQ2)

We first expand Eq. (1) for elective RAS using the coded inputs $w = (0.28, 0.26, 0.14, 0.08, 0.24)$ and $s = (0.86, 0.82, 0.55, 0.40, 0.72)$:

$$w_1 s_1 = 0.28 \times 0.86 = 0.2408, \tag{8}$$

$$w_2 s_2 = 0.26 \times 0.82 = 0.2132, \tag{9}$$
$$w_3 s_3 = 0.14 \times 0.55 = 0.0770, \tag{10}$$
$$w_4 s_4 = 0.08 \times 0.40 = 0.0320, \tag{11}$$
$$w_5 s_5 = 0.24 \times 0.72 = 0.1728, \tag{12}$$
$$R^{(\text{elective})} = 0.2408 + 0.2132 + 0.0770 + 0.0320 + 0.1728 = 0.7358 \approx 0.736. \tag{13}$$

The same expansion for XR training and teleoperation yields

$$R^{(\text{XR training})} = 0.12 \cdot 0.60 + 0.10 \cdot 0.48 + 0.38 \cdot 0.78 + 0.08 \cdot 0.42 + 0.32 \cdot 0.70 = 0.674, \tag{14}$$
$$R^{(\text{teleoperation})} = 0.22 \cdot 0.74 + 0.18 \cdot 0.70 + 0.16 \cdot 0.62 + 0.24 \cdot 0.48 + 0.20 \cdot 0.58 = 0.619. \tag{15}$$

Relative to the illustrative threshold $\tau = 0.70$, elective RAS meets the model threshold ($0.736 \geq 0.70$), XR training lies near it ($0.674 < 0.70$), and teleoperation remains below it ($0.619 < 0.70$) under the coded inputs (Fig. 5; Table 4). These labels are scenario-model outputs rather than clinical determinations.

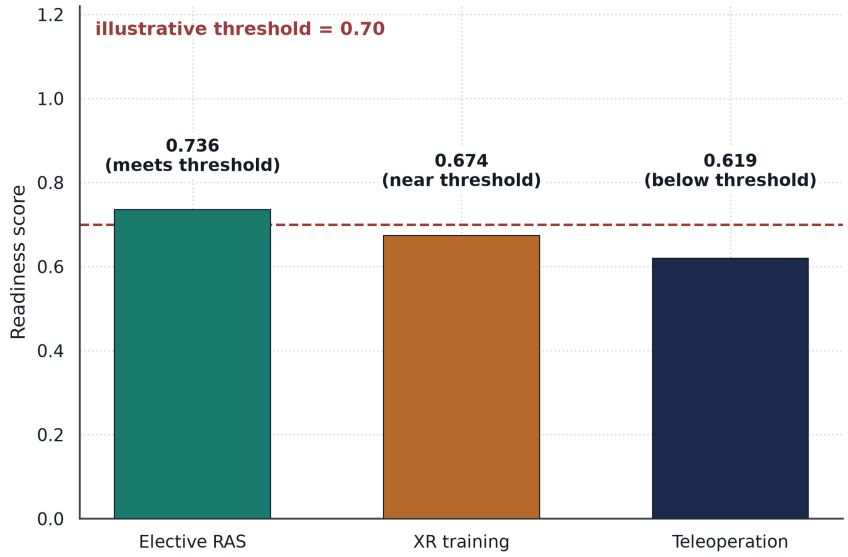


Fig. 5 Illustrative readiness scores $R^{(c)}$ versus model threshold $\tau = 0.70$ (Eq. (2)); labels are scenario-model comparisons, not clinical determinations.

3.3 Threshold sensitivity

Because τ is author-chosen, we re-evaluate the same coded point estimates against $\tau \in \{0.60, 0.65, 0.70, 0.75, 0.80\}$ (Table 5; Fig. 6). Elective RAS meets every $\tau \leq 0.70$

Table 4 Layer contributions $w_i s_i$ and total readiness by scenario

Scenario	L_1	L_2	L_3	L_4	L_5	$R^{(c)}$
Elective RAS	0.241	0.213	0.077	0.032	0.173	0.736
XR training	0.072	0.048	0.296	0.034	0.224	0.674
Teleoperation	0.163	0.126	0.099	0.115	0.116	0.619

and falls below $\tau \geq 0.75$. XR training meets $\tau \leq 0.65$ and falls below $\tau \geq 0.70$. Teleoperation meets only $\tau = 0.60$ among the tested values and remains below all higher cutoffs. Across this range, the comparative ordering elective RAS > XR training > teleoperation is unchanged, and teleoperation continues to lag elective RAS.

Table 5 Whether each coded scenario meets illustrative thresholds τ (M = meets; B = below)

Scenario	$\tau = 0.60$	0.65	0.70	0.75	0.80
Elective RAS ($R = 0.736$)	M	M	M	B	B
XR training ($R = 0.674$)	M	M	B	B	B
Teleoperation ($R = 0.619$)	M	B	B	B	B

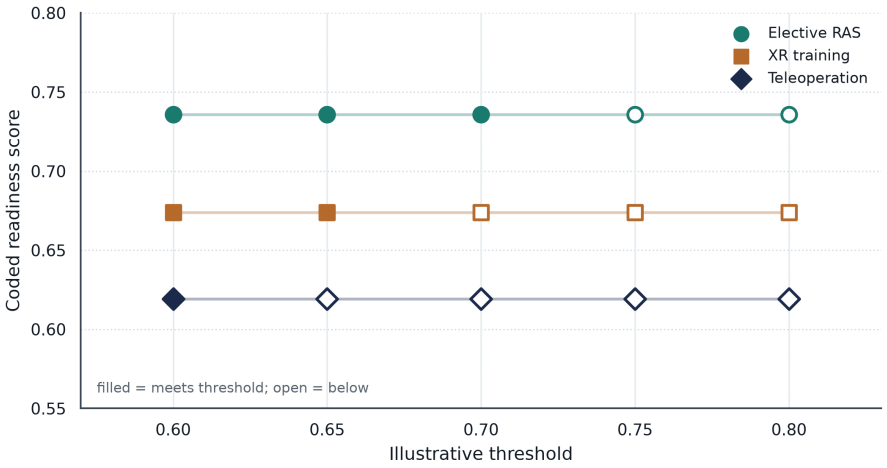


Fig. 6 Coded point readiness versus illustrative thresholds $\tau \in [0.60, 0.80]$. Markers denote meets (filled) or below (open).

Elective RAS draws most of its score from console and instrument layers, consistent with mature master-slave platforms, anatomic robotic techniques, and flexible-access

roadmaps [3, 9, 13, 20, 40]. XR training is dominated by L_3 and L_5, matching evidence that criterion-based VR rehearsal can transfer to the OR [2, 4], while broader AR/VR and metaverse education reviews still report uneven validation [12, 14, 25, 37, 38]. Demonstration learning and VR teleoperation pipelines further raise L_3 potential when RCM-safe skill models are available [19, 33]. Teleoperation spreads contribution across layers but remains limited by modest s_4 despite elevated w_4, consistent with delay stability, haptics, human-factor, and autonomy barriers [1, 5, 7, 23, 34, 41]. Randomized RAS trials and overviews further remind programs that diffusion [29] is not the same as superiority on every endpoint [10, 11, 17, 21, 24, 28, 32, 42].

3.4 Local and Dirichlet weight sensitivity for teleoperation

For teleoperation, each weight is perturbed by ± 0.05 and renormalized,

$$w \leftarrow \frac{w + \delta e_i}{\|w + \delta e_i\|_1}, \qquad \delta = \pm 0.05, \tag{16}$$

and the change $\Delta R = R(w) - R(w_{\text{base}})$ is recorded (Fig. 7). As a worked step for the network layer with $\delta = +0.05$,

$$w' = (0.22, 0.18, 0.16, 0.29, 0.20), \qquad \|w'\|_1 = 1.05, \tag{17}$$

$$w = w'/1.05 = (0.2095, 0.1714, 0.1524, 0.2762, 0.1905), \tag{18}$$

$$R = 0.6126, \qquad \Delta R = 0.6126 - 0.6192 = -0.0066. \tag{19}$$

Increasing the network weight can lower R after renormalization when s_4 is below the weighted average of the other scores; decreasing network weight raises R in the opposite move ($\Delta R \approx +0.0073$). Console-weight increases raise readiness ($\Delta R \approx +0.0058$).

In addition to one-at-a-time moves, we draw $N = 4000$ Dirichlet weights around each scenario base vector, $w \sim \text{Dirichlet}(\alpha w^{(c)})$ with concentration $\alpha = 40$, and recompute $R^{(c)}$. Under $\tau = 0.70$, the share of draws meeting the threshold is approximately 0.94 (elective RAS), 0.07 (XR training), and 0.00 (teleoperation). This joint weight uncertainty analysis agrees with the point-estimate ranking and with the local sensitivity in Fig. 7: teleoperation decisions remain brittle in L_4 under the present coding.

4 Surrogate Ranking, Uncertainty, and Upgrade Analysis

Section 3 established point estimates for RQ2. This section strengthens those answers with Monte Carlo uncertainty on $P(R \geq \tau)$, Sobol ranking of teleoperation layers, upgrade prioritization, and an illustrative feature-ranking visualization.

4.1 Scenario profiles and contribution structure

Figure 8 shows layer-score radar profiles: elective RAS is strong on console and instruments; XR training peaks on vision/XR and governance; teleoperation is flatter but

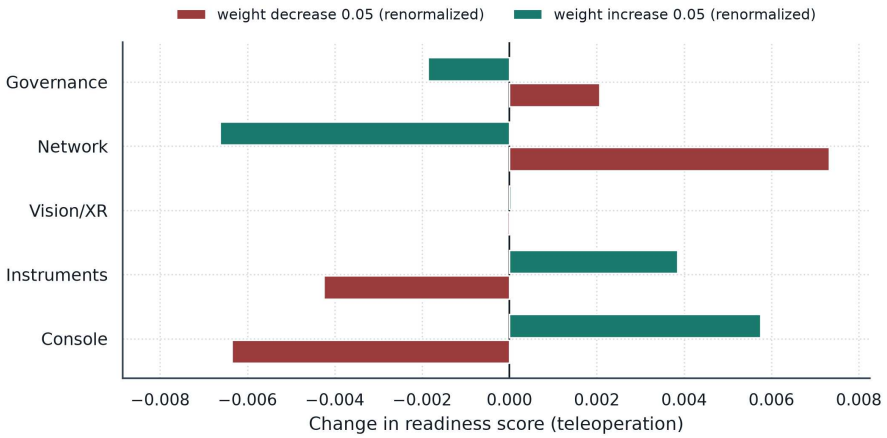


Fig. 7 One-at-a-time teleoperation weight sensitivity (± 0.05 then renormalize) showing change in readiness R.

weakest on network. Figure 9 decomposes $w_i s_i$ contributions, confirming that elective readiness is carried by L_1–L_2–L_5, XR training by L_3–L_5, and teleoperation by a more even but lower-valued mix. Figure 10 situates the same layers as a cyber-physical dependency graph from surgeon and governance through console, vision, instruments, and network to the patient/OR.

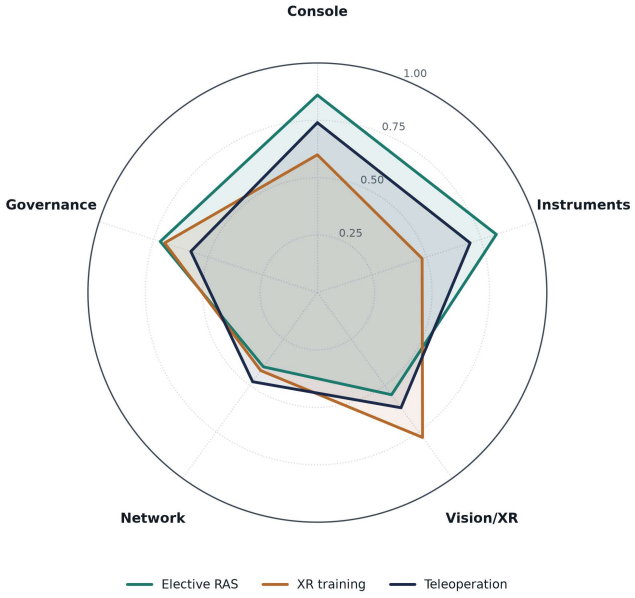


Fig. 8 Layer-score radar profiles for elective RAS, XR training, and teleoperation.

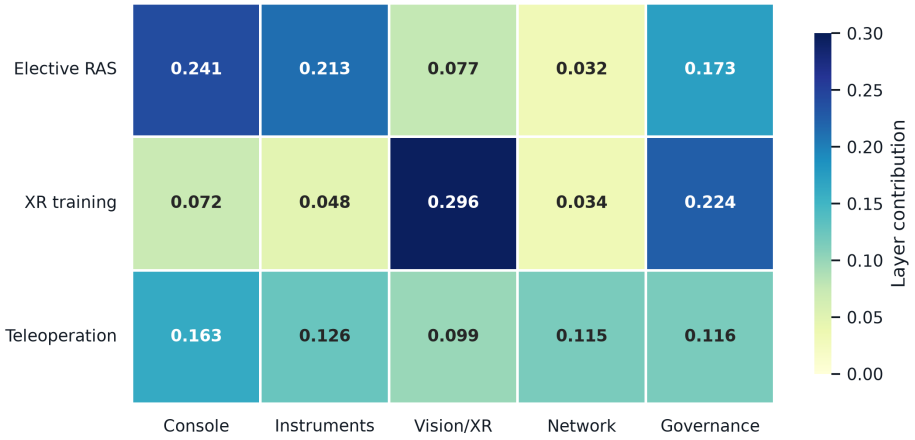


Fig. 9 Heatmap of layer contributions $w_i s_i$ by scenario (Eq. (1)).

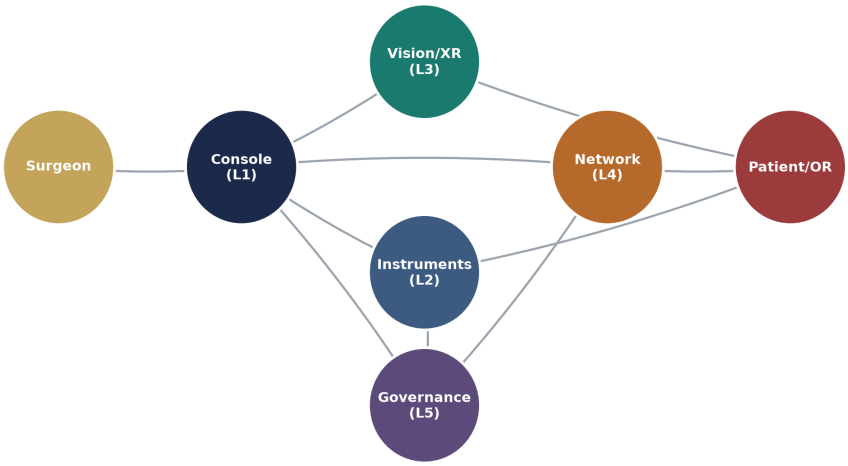


Fig. 10 Cyber-physical dependency graph of the robotic OR readiness stack.

4.2 Monte Carlo uncertainty on layer scores

Point estimates of $R^{(c)}$ ignore coding noise. As an *illustrative* uncertainty analysis we draw $N = 4000$ Monte Carlo samples with

$$s_i^{(c,\nu)} = \mathrm{clip}_{[0,1]}\left(s_i^{(c)} + \varepsilon_i^{(\nu)}\right), \qquad \varepsilon_i^{(\nu)} \sim \mathcal{N}(0, \sigma^2), \quad \sigma \in \{0.02, 0.04, 0.06\}, \tag{20}$$

and recompute $R^{(c,\nu)} = \sum_i w_i^{(c)} s_i^{(c,\nu)}$ (random seed fixed in the accompanying script). Table 6 and Fig. 11 summarize the baseline case $\sigma = 0.04$. Elective RAS remains

almost surely above $\tau = 0.70$ ($P(R \geq \tau) \approx 0.97$), XR training straddles the threshold ($P \approx 0.11$), and teleoperation remains below τ in essentially all draws ($P \approx 0$). Repeating with $\sigma = 0.02$ and $\sigma = 0.06$ yields elective $P \approx 1.00$ and 0.89, XR $P \approx 0.01$ and 0.21, and teleoperation $P \approx 0.00$ in both cases (Table 7). Noise magnitude changes the absolute probabilities but not the comparative conclusion that teleoperation lags elective RAS under these coded inputs.

Table 6 Monte Carlo readiness summary (illustrative $\sigma = 0.04$, $N = 4000$, seed fixed)

Scenario	Mean R	5th–95th pct.	$P(R \geq \tau)$	Point R
Elective RAS	0.736	0.704–0.768	0.968	0.736
XR training	0.674	0.640–0.709	0.111	0.674
Teleoperation	0.619	0.589–0.648	0.000	0.619

Table 7 Monte Carlo $P(R \geq 0.70)$ under illustrative score noise σ ($N = 4000$)

Scenario	$\sigma = 0.02$	0.04	0.06
Elective RAS	1.000	0.968	0.891
XR training	0.007	0.111	0.213
Teleoperation	0.000	0.000	0.001

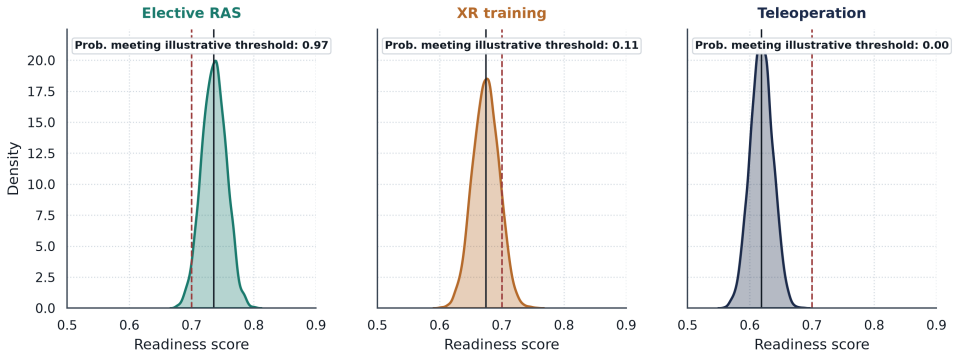


Fig. 11 Kernel density estimates of illustrative Monte Carlo readiness under layer-score noise ($\sigma = 0.04$ in Eq. (20)). Dashed line: $\tau = 0.70$; panel annotations report $P(R \geq \tau)$.

4.3 Global sensitivity and upgrade prioritization

Beyond local weight perturbations (Fig. 7), we compute exact first-order Sobol indices for the linear teleoperation model under equal score variance,

$$S_i = \frac{w_i^2}{\sum_{j=1}^{5} w_j^2}, \tag{21}$$

shown in Fig. 12. Network ($S_4 = 0.282$) and console ($S_1 = 0.237$) dominate score-driven variance, followed by governance (0.196), instruments (0.159), and vision/XR (0.125). A practical upgrade tornado (Fig. 13) asks: if any single layer score improves by $+0.10$, how much does teleoperation R rise? Network yields the largest gain ($\Delta R = +0.024$), then console ($+0.022$), governance ($+0.020$), instruments ($+0.018$), and vision/XR ($+0.016$). Even the best single-layer upgrade leaves teleoperation below τ ($R \approx 0.643$), which is why the binary gate G remains essential.

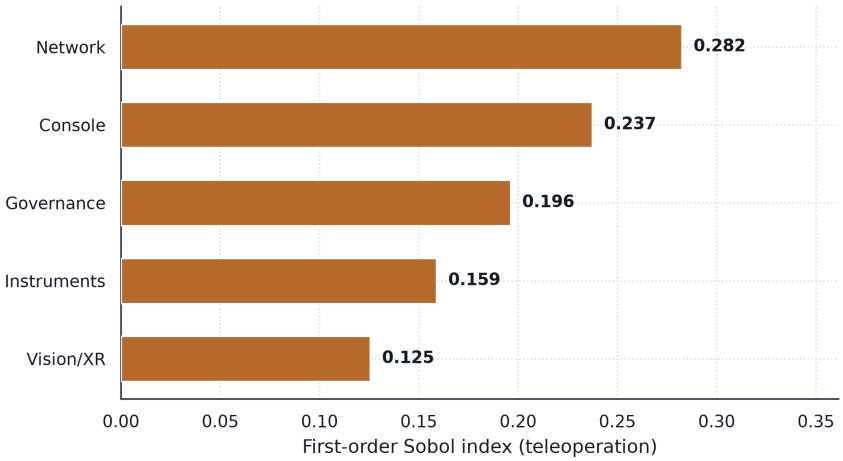


Fig. 12 Teleoperation first-order Sobol indices under equal layer-score variance, $S_i = w_i^2 / \sum_j w_j^2$ (Eq. (21)).

4.4 Illustrative ridge ranking (not a predictive classifier)

To connect the multi-criteria score to an explicit ranking view, we build an *illustrative* ridge ranking on six engineering features $f =$ (control fidelity, instrument dexterity, XR registration, network RTT adequacy, credential coverage, fail-safe cov
Feature values follow the corresponding layer scores, with an explicit fail-safe coordinate coded lower for teleoperation. Labels are $y = \mathbf{1}[R^{(c)} \geq \tau]$. Because only three nominal scenarios are available, we expand the design with bootstrap noise around

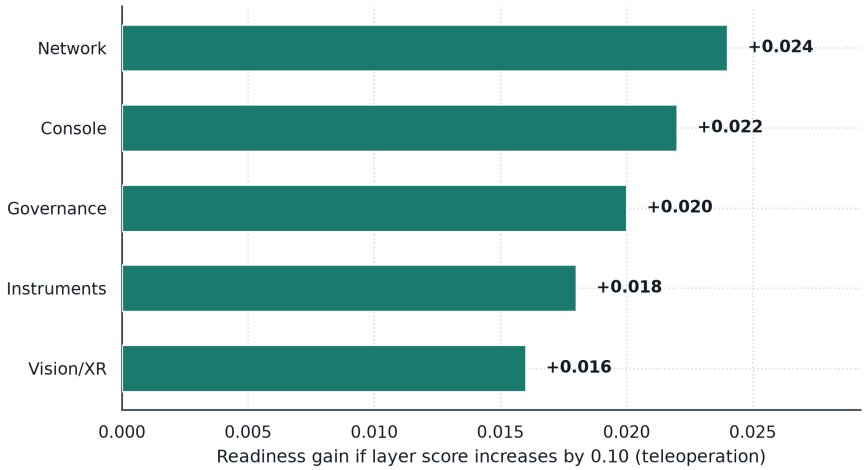


Fig. 13 Tornado plot of readiness change ΔR for a +0.10 teleoperation layer-score upgrade.

the coded points ($n = 363$ rows) and solve

$$\min_{\beta} \ \|y - F\beta\|_2^2 + \lambda\|\beta\|_2^2, \qquad \lambda = 10^{-2}, \tag{22}$$

after standardizing columns. Normalized ridge importances

$$\iota_j = \frac{|\hat{\beta}_j|}{\sum_{k=1}^{6} |\hat{\beta}_k|} \tag{23}$$

and permutation importances are reported in Table 8 and Fig. 14. Instrument dexterity and fail-safe coverage dominate both rankings, with control fidelity next; network RTT is weaker in the surrogate because above-/below-threshold labels are already separated strongly by instrument/fail-safe coordinates under the coded scenarios. This does *not* contradict the teleoperation weight sensitivity in L_4: the gate G and upgrade tornado still prioritize network assurance for remote pathways, while the surrogate is only an illustrative ranking visualization of which features most separate above-threshold versus below-threshold prototypes in a bootstrap-expanded cloud of three scenario points. We do not report fit R^2 as evidence of predictive validity.

Table 8 Normalized ridge and permutation importances for illustrative feature ranking ($\lambda = 10^{-2}$, bootstrap-expanded design; not a clinical classifier)

Feature	Control	Instruments	XR reg.	Network RTT	Credential	Fail-safe
Ridge ι_j	0.165	0.295	0.111	0.030	0.113	0.286
Perm. ι_j	0.122	0.390	0.055	0.004	0.057	0.372

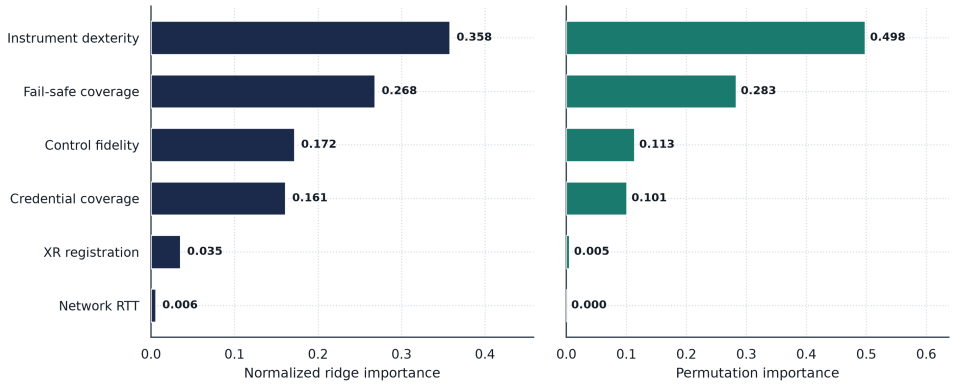


Fig. 14 Illustrative ridge and permutation feature ranking on bootstrap-expanded scenario prototypes (Eq. (22)); not a predictive clinical classifier.

Remark 1 The surrogate and Monte Carlo analyses are transparency tools on literature-coded indicators. They are not predictive classifiers, clinical decision algorithms, or multi-center validated models.

5 Discussion, Limitations, and Applications

5.1 Answers to the research questions

RQ1 answer.

Robotic OR capability is formalized as Eq. (1): a convex combination of five layer scores with scenario-dependent weights, an illustrative model threshold $\tau = 0.70$ (Eq. (2)), and, for remote pathways, a scenario-model latency parameter plus binary AND gate G (Eqs. (4)–(5); Table 3). The formulation is transparent, bounded, and monotone (Section 3.1).

RQ2 answer.

Under the literature-coded inputs and illustrative $\tau = 0.70$, elective RAS meets the model threshold ($R = 0.736$; Monte Carlo $P(R \geq \tau) \approx 0.97$), XR training lies near it ($R = 0.674$; $P \approx 0.11$), and teleoperation remains below it ($R = 0.619$; $P \approx 0$) and additionally fails G. These are scenario-model outputs, not clinical determinations. Teleoperation sensitivity and Sobol indices identify network and console as high-leverage layers for remote pathways; the illustrative surrogate ranking highlights instrument dexterity and fail-safe coverage among features that separate above- versus below-threshold prototypes.

5.2 Clinical interpretation

Under the stated inputs, elective RAS clears τ because console and instrument layers are comparatively mature [3, 13, 20]. Soft, continuum, and flexible robots can raise future s_2 for delicate or single-port anatomy, but sterilization, sensing, control,

locomotion in confined spaces, and clinical validation remain incomplete relative to rigid platforms [18, 22, 26, 30, 31, 35, 36, 40, 43]. XR robotic training sits near the threshold: classic VR transfer evidence and skills-lab pedagogy are encouraging [2, 4], yet broader AR/VR/metaverse education reviews still report mixed validation and access barriers [12, 14, 25, 37, 38]. Teaching-by-demonstration and VR-imitation pipelines can further couple L_3 to future semi-autonomous assistance if RCM safety is preserved [19, 33].

Remote teleoperation remains below τ and fails G primarily because network assurance, haptics transparency, supervised autonomy, human-factor mitigations, and fail-safe coverage are incomplete relative to clinical risk [1, 5, 7, 23, 34, 41, 44]. AR and VR tools should be judged by educational or guidance endpoints rather than display novelty alone [12, 25]. In the model, that requirement appears as pressure on s_3; poor registration or weak transfer cannot be rescued by raising console weight. Clinical RCTs, functional meta-analyses, and overview-of-reviews syntheses likewise argue for explicit readiness tracking before further diffusion [9–11, 17, 21, 24, 28, 29, 32, 42]. When scoring L_5, programs can borrow the discipline of endpoint-linked training intensity from adjacent robot-mediated therapy literature without treating those trials as surgical outcome evidence [6, 8, 27].

5.3 Link to outcomes robotic programs already track

Readiness $R^{(c)}$ is not itself a patient outcome. Table 9 maps layers to endpoints commonly reported in robotic programs so that sites can replace author codes with local audit data over time.

Table 9 Suggested outcome anchors for each layer when replacing author codes with institutional data

Layer	Example process metrics	Example clinical/training endpoints
L_1 Console	Console fault rate; ergonomic incident logs	Conversion attributable to visualization/control
L_2 Instruments	Instrument collision/exchange time; soft-tool availability	Precision-related complications; access conversions
L_3 Vision/XR	Registration error (mm); VR curriculum completion	Skill-transfer scores; guidance-related near misses
L_4 Network	Measured ℓ; packet loss; failover test pass rate	Remote-case abort rate; safety freezes
L_5 Governance	Credential roster coverage; cyber patch lag	Training compliance; audit findings

5.4 Applications for robotic programs

Programs can use Eq. (1) as a pre-deployment checklist: encode local weights for their case mix (e.g., raise w_3 for XR-heavy onboarding of new robotic surgeons),

score layers from equipment audits and credentialing records, compare $R^{(c)}$ with the chosen illustrative τ, and refuse remote pathways in the model unless $G = 1$ and $\ell \leq \ell_{\max}$. Monte Carlo $P(R \geq \tau)$ and Dirichlet weight draws quantify illustrative coding/weight uncertainty; the upgrade tornado and local weight sensitivity identify which investment (network SLA, fail-safe testing, XR curriculum, or console training) most improves the model score per scenario. The framework is a transparent program-level decision aid, not a validated clinical prediction model or regulatory score.

5.5 Limitations

Weights and layer scores are literature-informed author codes anchored to the curated corpus; they are a preliminary proof-of-concept, not multi-rater Delphi estimates or hospital telemetry, and no inter-rater agreement statistics are reported here. The threshold $\tau = 0.70$ and latency parameter $\ell_{\max} = 150$ ms are illustrative scenario-model aids, not validated clinical standards. Growth rate $\hat{g}$ summarizes two published endpoints and does not forecast future adoption [29]. Monte Carlo noise ($\sigma = 0.02$–0.06) and Dirichlet weight draws are illustrative uncertainty analyses. The bootstrap ridge ranking expands only three scenario prototypes and must not be read as a predictive classifier. Specialty-specific RAS endpoints should be linked to s_i in future multi-center work [10, 11, 17, 21, 24, 28, 32, 42]. Soft-robot translational gaps remain [26, 36, 40].

6 Conclusion

We presented a five-layer CPS readiness framework for RAS with an explicit index $R^{(c)}$, illustrative threshold τ, teleoperation gate G, adoption-growth statistic, threshold/weight/noise sensitivity, Monte Carlo uncertainty, upgrade prioritization, and an illustrative ridge/permutation feature ranking.

RQ1.

Readiness is a convex combination of console, instrument, vision/XR, network, and governance scores with scenario-dependent weights (Section 2).

RQ2.

Under the coded illustrative inputs and $\tau = 0.70$, elective RAS meets the model threshold ($R = 0.736$, $P(R \geq \tau) \approx 0.97$), XR training lies near it ($R = 0.674$, $P \approx 0.11$), and teleoperation remains below it ($R = 0.619$, $P \approx 0$) and fails G. Network assurance and fail-safe coverage dominate remote-pathway leverage in the sensitivity analyses (Sections 3–4). These statements are transparent program-planning outputs, not validated clinical scores.

Future work should replace author codes with multi-rater or institutional measurements, link layers to specialty-specific outcomes, and preserve the transparent equation-level structure required for surgical program decisions.

Acknowledgements

The authors thank colleagues who provided feedback on earlier drafts of this manuscript.

Declarations

- Funding: The authors declare that no funds, grants, or other support were received during the preparation of this manuscript.
- Competing interests: The authors have no relevant financial or non-financial interests to disclose.
- Ethics approval and consent to participate: Not applicable. This article develops a modeling and secondary-data analysis framework and does not report studies involving human participants or animals performed by the authors.
- Consent for publication: Not applicable.
- Data availability: All indicator codes, scenario weights, layer-score calculations, gate conditions, threshold values, Monte Carlo settings (including random seed), sensitivity scripts, and figure-generation code are reported in the figures/tables of this article and in the accompanying analysis export (`analysis_results.json` and `regen_jors_figures.py`). Adoption endpoints are taken from Sheetz *et al.* No primary patient-level datasets were generated.
- Materials availability: Not applicable.
- Code availability: Figure-generation and analysis code (NumPy/SciPy/scikit-learn/Seaborn/NetworkX) is included with the submission materials and is also available from the corresponding author on request.
- Author contribution: U.A. conceived the study, formulated the readiness model, performed the numerical analysis, prepared the figures and tables, and wrote the main manuscript text. M.A. contributed to indicator coding, result checking, and critical revision. S.K.K. contributed to clinical framing, narrative revision, and manuscript editing. All authors reviewed the manuscript and approved the final version.

References

[1] Niemeyer G, Slotine JJE (1991) Stable adaptive teleoperation. IEEE J Oceanic Eng 16(1):152-162. https://doi.org/10.1109/48.64895

[2] Seymour NE, Gallagher AG, Roman SA, O'Brien MK, Bansal VK, Andersen DK, Satava RM (2002) Virtual reality training improves operating room performance: results of a randomized, double-blinded study. Ann Surg 236(4):458-463. https://doi.org/10.1097/00000658-200210000-00008

[3] Lanfranco AR, Castellanos AE, Desai JP, Meyers WC (2004) Robotic surgery: a current perspective. Ann Surg 239(1):14-21. https://doi.org/10.1097/01.sla.0000103020.19595.7d

[4] Reznick RK, MacRae H (2006) Teaching surgical skills: changes in the wind. N Engl J Med 355(25):2664-2669. https://doi.org/10.1056/NEJMra054785

[5] Chen JYC, Haas EC, Barnes MJ (2007) Human performance issues and user interface design for teleoperated robots. IEEE Trans Syst Man Cybern Part C Appl Rev 37(6):1231-1245. https://doi.org/10.1109/TSMCC.2007.905819

[6] Kwakkel G, Kollen BJ, Krebs HI (2008) Effects of robot-assisted therapy on upper limb recovery after stroke: a systematic review. Neurorehabil Neural Repair 22(2):111-121. https://doi.org/10.1177/1545968307305457

[7] Okamura AM (2009) Haptic feedback in robot-assisted minimally invasive surgery. Curr Opin Urol 19(1):102-107. https://doi.org/10.1097/MOU.0b013e32831a478c

[8] Lo AC, Guarino PD, Richards LG, et al (2010) Robot-assisted therapy for long-term upper-limb impairment after stroke. N Engl J Med 362(19):1772-1783. https://doi.org/10.1056/NEJMoa0911341

[9] Galfano A, Ascione A, Grimaldi S, Petralia G, Strada E, Bocciardi AM (2010) A new anatomic approach for robot-assisted laparoscopic prostatectomy: a feasibility study for completely intrafascial surgery. Eur Urol 58(3):457-461. https://doi.org/10.1016/j.eururo.2010.06.008

[10] Ficarra V, Novara G, Rosen RC, et al (2012) Systematic review and meta-analysis of studies reporting urinary continence recovery after robot-assisted radical prostatectomy. Eur Urol 62(3):405-417. https://doi.org/10.1016/j.eururo.2012.05.045

[11] Yaxley JW, Coughlin GD, Chambers SK, et al (2016) Robot-assisted laparoscopic prostatectomy versus open radical retropubic prostatectomy: early outcomes from a randomised controlled phase 3 study. Lancet 388(10049):1057-1066. https://doi.org/10.1016/S0140-6736(16)30592-X

[12] Barsom EZ, Graafland M, Schijven MP (2016) Systematic review on the effectiveness of augmented reality applications in medical training. Surg Endosc 30:4174-4183. https://doi.org/10.1007/s00464-016-4800-6

[13] Ghezzi TL, Corleta OC (2016) 30 years of robotic surgery. World J Surg 40(10):2550-2557. https://doi.org/10.1007/s00268-016-3543-9

[14] Li L, Yu F, Shi D, Shi J, Tian Z, Yang J, Wang X, Jiang Q (2017) Application of virtual reality technology in clinical medicine. Am J Transl Res 9(9):3867-3880

[15] Nam KY, Kim HJ, Kwon BS, Park JW, Lee HJ, Yoo A (2017) Robot-assisted gait training (Lokomat) improves walking function and activity in people with spinal cord injury: a systematic review. J Neuroeng Rehabil 14:24. https://doi.org/10.1186/s12984-017-0232-3

[16] Bertani R, Melegari C, De Cola MC, Bramanti A, Bramanti P, Calabrò RS (2017) Effects of robot-assisted upper limb rehabilitation in stroke patients: a systematic review with meta-analysis. Neurol Sci 38:1561-1569. https://doi.org/10.1007/s10072-017-2995-5

[17] Jayne D, Pigazzi A, Marshall H, et al (2017) Effect of robotic-assisted vs conventional laparoscopic surgery on risk of conversion to open laparotomy among patients undergoing resection for rectal cancer: the ROLARR randomized clinical trial. JAMA 318(16):1569-1580. https://doi.org/10.1001/jama.2017.7219

[18] Gorissen B, Reynaerts D, Konishi S, Yoshida K, Kim JW, De Volder M (2017) Elastic inflatable actuators for soft robotic applications. Adv Mater 29(43):1604977. https://doi.org/10.1002/adma.201604977

[19] Zhang T, McCarthy Z, Jow O, Lee D, Chen X, Goldberg K, Abbeel P (2018) Deep imitation learning for complex manipulation tasks from virtual reality teleoperation. In: Proc IEEE Int Conf Robot Autom (ICRA), pp 5628-5635. https://doi.org/10.1109/ICRA.2018.8461249

[20] Peters BS, Armijo PR, Krause C, Choudhury SA, Oleynikov D (2018) Review of emerging surgical robotic technology. Surg Endosc 32:1636-1655. https://doi.org/10.1007/s00464-018-6079-2

[21] Coughlin GD, Yaxley JW, Chambers SK, et al (2018) Robot-assisted laparoscopic prostatectomy versus open radical retropubic prostatectomy: 24-month outcomes from a randomised controlled study. Lancet Oncol 19(8):1051-1060. https://doi.org/10.1016/S1470-2045(18)30357-7

[22] Cianchetti M, Laschi C, Menciassi A, Dario P (2018) Biomedical applications of soft robotics. Nat Rev Mater 3:143-153. https://doi.org/10.1038/s41578-018-0022-y

[23] Haidegger T (2019) Autonomy for surgical robots: concepts and paradigms. IEEE Trans Med Robot Bionics 1(2):65-76. https://doi.org/10.1109/TMRB.2019.2913282

[24] Nichols AC, Theurer J, Prisman E, et al (2019) Radiotherapy versus transoral robotic surgery and neck dissection for oropharyngeal squamous cell carcinoma (ORATOR): an open-label, phase 2, randomised trial. Lancet Oncol 20(10):1349-1359. https://doi.org/10.1016/S1470-2045(19)30410-3

[25] Kyaw BM, Saxena N, Posadzki P, Vseteckova J, Nikolaou CK, George PP, Divakar U, Masiello I, Kononowicz AA, Zary N, Tudor Car L (2019) Virtual reality for health professions education: systematic review and meta-analysis by the Digital Health Education Collaboration. J Med Internet Res 21(1):e12959. https://doi.org/10.2196/12959

[26] Runciman M, Darzi A, Mylonas GP (2019) Soft robotics in minimally invasive surgery. Soft Robot 6(4):423-443. https://doi.org/10.1089/soro.2018.0136

[27] Rodgers H, Bosomworth H, Krebs HI, et al (2019) Robot assisted training for the upper limb after stroke (RATULS): a multicentre randomised controlled trial. Lancet 394(10192):51-62. https://doi.org/10.1016/S0140-6736(19)31055-4

[28] van der Sluis PC, van der Horst S, May AM, et al (2019) Robot-assisted minimally invasive thoracolaparoscopic esophagectomy versus open transthoracic esophagectomy for resectable esophageal cancer: a randomized controlled trial. Ann Surg 269(4):621-630. https://doi.org/10.1097/SLA.0000000000003031

[29] Sheetz KH, Claflin J, Dimick JB (2020) Trends in the adoption of robotic surgery for common surgical procedures. JAMA Netw Open 3(1):e1918911. https://doi.org/10.1001/jamanetworkopen.2019.18911

[30] Kolachalama S, Lakshmanan S (2020) Continuum robots for manipulation applications: a survey. J Robot 2020:4187048. https://doi.org/10.1155/2020/4187048

[31] Ng CSX, Tan MWM, Xu C, Yang Z, Lee PS, Lum GZ (2020) Locomotion of miniature soft robots. Adv Mater 32:2003558. https://doi.org/10.1002/adma.202003558

[32] Muaddi H, El Hafid M, Choi WJ, Lillie E, de Mestral C, Nathens A, Stukel TA, Karanicolas PJ (2021) Clinical outcomes of robotic surgery compared to conventional surgical approaches (laparoscopic or open): a systematic overview of reviews. Ann Surg 273(3):467-473. https://doi.org/10.1097/SLA.0000000000003915

[33] Su H, Mariani A, Ovur SE, Menciassi A, Ferrigno G, De Momi E (2021) Toward teaching by demonstration for robot-assisted minimally invasive surgery. IEEE Trans Autom Sci Eng 18(2):484-494. https://doi.org/10.1109/TASE.2020.3045655

[34] Yang C, Peng G, Cheng L, Na J, Li Z (2021) Force sensorless admittance control for teleoperation of uncertain robot manipulator using neural networks. IEEE Trans Syst Man Cybern Syst 51(5):3282-3292. https://doi.org/10.1109/TSMC.2019.2920870

[35] Dou W, Zhong G, Cao J, Shi Z, Peng B, Jiang L (2021) Soft robotic manipulators: designs, actuation, stiffness tuning, and sensing. Adv Mater Technol 6(9):2100018. https://doi.org/10.1002/admt.202100018

[36] Zhu J, Lyu L, Xu Y, Liang H, Zhang X, Ding H, Wu Z (2021) Intelligent soft surgical robots for next-generation minimally invasive surgery. Adv Intell Syst 3(5):2100011. https://doi.org/10.1002/aisy.202100011

[37] Barteit S, Lanfermann L, Bärnighausen T, Neuhann F, Beiersmann C (2021) Augmented, mixed, and virtual reality-based head-mounted devices for medical education: systematic review. JMIR Serious Games 9(3):e29080. https://doi.org/10.2196/29080

[38] Kye B, Han N, Kim E, Park Y, Jo S (2021) Educational applications of metaverse: possibilities and limitations. J Educ Eval Health Prof 18:32. https://doi.org/10.3352/jeehp.2021.18.32

[39] Hussain S, Jamwal PK, van Vliet P, Brown NAT (2021) Robot assisted ankle neuro-rehabilitation: state of the art and future challenges. Expert Rev Neurother 21(1):111-121. https://doi.org/10.1080/14737175.2021.1847646

[40] Omisore OM, Han S, Xiong J, Li H, Li Z, Wang L (2022) A review on flexible robotic systems for minimally invasive surgery. IEEE Trans Syst Man Cybern Syst 52(1):631-644. https://doi.org/10.1109/TSMC.2020.3026174

[41] Saeidi H, Opfermann JD, Kam M, Wei S, Leonard S, Hsieh MH, Kang JU, Krieger A (2022) Autonomous robotic laparoscopic surgery for intestinal anastomosis. Sci Robot 7(62):eabj2908. https://doi.org/10.1126/scirobotics.abj2908

[42] Catto JWF, Khetrapal P, Ricciardi F, et al; iROC Study Team (2022) Effect of robot-assisted radical cystectomy with intracorporeal urinary diversion vs open radical cystectomy on 90-day morbidity and mortality among patients with bladder cancer: a randomized clinical trial. JAMA 327(21):2092-2103. https://doi.org/10.1001/jama.2022.7393

[43] Ze Q, Wu S, Nishikawa J, Dai J, Sun Y, Leanza S, Zullo R, Clark LM, Plott J, Liu N, et al (2022) Soft robotic origami crawler. Sci Adv 8(13):eabm7834. https://doi.org/10.1126/sciadv.abm7834

[44] Ali U, Salim O, Ahmed M, Kulsoom SK (2026) Two decades of Industry 4.0 and IoT research: A bibliometric analysis of global trends, market dynamics, and technological convergences (2004-2024). The USA Journals TAJET 8(3):39-69. https://usajournal.net/index.php/tujtajet/article/view/1243